Research Article

Characterization and Photocatalytic Activity of TiO$_2$ Nanotube Films Prepared by Anodization

Wen-Yu Wang and Bo-Ruei Chen

Department of Environmental Engineering and Management, Chaoyang University of Technology, 168, Jifeng E. Rd.,
Wufeng District, Taichung 41349, Taiwan

Correspondence should be addressed to Wen-Yu Wang; wywang@cyut.edu.tw

Titanium dioxide nanotube (TNT) arrays were prepared in electrolytes containing fluoride by anodic oxidation. Different preparation parameters were investigated in order to evaluate their effects on length and inner diameter of nanotube, including weight ratio of glycerol to water, anodization voltage, electrolysis time, bath temperature, and electrolyte solution pH. The well defined and highly ordered TNT arrays were formed in electrolyte containing 40, and 20% water. The inner diameter of TNT was observed to increase as anodization voltage increased across the range of 10–40 V. The length of TNT was affected simultaneously by both anodization voltage and electrolysis time. The inner diameter and length depend on bath temperature below 60°C. The morphology of TNT was well defined and highly ordered only at electrolyte solution pH of 6 across the pH range of 2–10. Photocatalysis of methylene blue showed that reaction rate constants by TNT films were higher than P-25 films at comparable thickness. Reaction rate constants by TNT films increased as film thickness increased, but the enhancement was retarded when the length of TNT reached 2200 nm which appeared to be the limited penetration of incident UV light.

1. Introduction

In the past decade, considerable attention has been focused on using nanocrystalline TiO$_2$ as a photocatalyst for the degradation of organic pollutants [1]. The photocatalyst titanium dioxide is a wide bandgap semiconductor, corresponding to radiation in the near-UV range. An electron-hole pair formation occurs within the conduction and valence bands of TiO$_2$ after the absorption of UV radiation. The positive hole is apparently able to oxidize a water molecule to hydroxyl radical [2]. The hydroxyl radical, in turn, is a powerful oxidant. The oxidation of organic contaminants seems to be mediated by a series of reactions initiated by hydroxyl radical on the TiO$_2$ surface. However, recombination of the separated electron and hole can occur either in the volume or on the surface of the semiconductor particle accompanied with heat releasing [3].

Highly ordered TiO$_2$ nanotube (TNT) arrays have been regarded as potential superior photocatalyst due to their valuable high surface area structure. The one-dimensional nanostructures with tubular symmetries possessed low recombination of light-induced electron-hole pairs and high photocurrent conversion efficiency [4]. Quan et al. [5], and Wang et al. [6] indicated that TNT attached to the parent titanium substrate improved the transport of the photo-induced electrons from photoanode to cathode and enhanced the photocatalytic activity of TNT.

In recent years, numerous researchers have paid their attention on developing new techniques for fabrication of TNT, such as template [7], hydrothermal [8] and anodic oxidation method [9]. The electrochemical oxidization and chemical dissolution rates of TiO$_2$ were the keys to fabricate TNT by anodic oxidation method. The thin layer of TiO$_2$ was formed on the titanium surface in the onset of anodization. The pores could be observed on the surface of TiO$_2$ layer after the localized dissolution of the TiO$_2$ by fluoride ions. When the pores became deeper, the electric field at the bottom of pores was increased to enhance the electrochemical oxidization and chemical dissolution rates of TiO$_2$ and to form the tubular structure of TiO$_2$. The length

of TNT remained constant when electrochemical oxidization rate and chemical dissolution rate reached dynamic balance [10].

Although various studies on the preparation of TNT had been reported, this study widely investigated the effects of various preparation parameters on length and inner diameter of TNT. These parameters included weight ratio of glycerol to water, anodization voltage, electrolysis time, bath temperature, and electrolyte solution pH. Photocatalytic efficiency was affected by diameter and length of TNT. Alivov and Fan [11] reported on the performance of dye sensitized solar cells (DSSCs) based on different diameters of TNT filled with TiO_2 nanoparticles. It is shown that the efficiency of DSSCs significantly increased with relative increasing of diameter of TNT. Macák et al. [4] revealed that higher light-induced photocurrent can be achieved by TNT with longer tube length.

As to our knowledge there was comparatively little research on the preparation parameter of electrolyte solution pH and the comparison of photocatalysis efficiency among comparable thickness of TNT films and P-25 films. In order to examine the relation between photocatalysis rate and the length of TNT film, photocatalytic reactions of methylene blue with various thicknesses of TNT and P-25 films were also performed.

2. Experimental

2.1. Preparation and Characterization of TiO₂ Nanotube Arrays.

A 25 × 15 mm Ti foil (99.53%) was subsequently immersed in acetone, isopropanol, methanol and deionized water for 10 minutes to remove the impurities and then dried at room temperature. Ti and Pt foils connected by Pt wire were used as anode and cathode, respectively. The glycerol solution containing 0.5 wt% NH_4F and water content ranging from 0 to 90 wt% was used as electrolyte and transferred to an electrolytic reactor along with electrodes for the anodization of Ti foil. Anodization voltage and electrolysis time were controlled by a programmable DC power supply (CDP-350-005PB, Chyng Hong Electronic) across the range of 10–70 V and 1–8 hours, respectively. Bath temperature was controlled via a water jacket with a thermostatic circulating water bath (BL-720, Yihder Technology). Electrolyte solution pH was adjusted among 2 to 10. The complete preparation parameters are listed in Table 1. The anodized Ti foils were put into a muffle furnace at different temperatures ranged from 200 to 800°C for 3 hours to induce crystallization. Because of the TNT films calcined at 600°C presented the best photocatalytic activity (as experimental procedure described in Section 2.2), the calcination temperature of 600°C was chosen in all experiments in this study. The surface dimensions of anodized Ti foil were determined by a field-emission scanning electron microscopy (JSM-6500F, JEOL).

2.2. Photocatalytic Activity Tests.

The photocatalytic reaction system was composed of a photoreactor, UV-LED lamp,

Table 1: Experimental design matrix for preparation of TNT.

Weight ratio of glycerol to water	Anodization voltage (V)	Electrolysis time (hours)	Bath temperature (°C)	Electrolyte solution pH
1 : 9	30	2	40	6
2 : 8	30	2	40	6
4 : 6	30	2	40	6
6 : 4	30	2	40	6
8 : 2	30	2	40	6
10 : 0	30	2	40	6
6 : 4	10	2	40	6
6 : 4	20	2	40	6
6 : 4	40	2	40	6
6 : 4	50	2	40	6
6 : 4	60	2	40	6
6 : 4	70	2	40	6
6 : 4	30	1	40	6
6 : 4	30	4	40	6
6 : 4	30	6	40	6
6 : 4	30	8	40	6
6 : 4	30	10	40	6
6 : 4	30	2	10	6
6 : 4	30	2	20	6
6 : 4	30	2	50	6
6 : 4	30	2	60	6
6 : 4	30	2	80	6
6 : 4	30	2	40	2
6 : 4	30	2	40	4
6 : 4	30	2	40	8
6 : 4	30	2	40	10

dye solution flask, peristaltic pump, and UV-Vis spectrophotometer and operated in recirculation mode. Silicone pipes connected the above equipment for circulation of the dye solution. The peristaltic pump transported methylene blue solution from the dye solution flask to photoreactor and recycled back to the dye solution flask. Major components of the photoreactor were made entirely of teflon. The photoreactor contained two hollow fillisters at the top fixture and the bottom fixture, respectively. The photocatalyst film (TNT or Degussa P-25) was attached under the top fixture. A quartz plate was mounted on the bottom fixture to penetrate the UV light. A UV-LED lamp with wavelength of 365 nm and irradiation power of $2\,mW/cm^2$ was put under the photoreactor. Dye solution was pumped through the flow channel hold between the top fixture and the bottom fixture. The initial concentration of methylene blue solution was 10 mg/L for all experiments. The photocatalytic reactions were carried out with various thicknesses of TNT and P-25 films. The TNT films were prepared by anodic oxidation method, and the P-25 films were prepared by dipcoating of suspension [12]. Concentrations of methylene blue
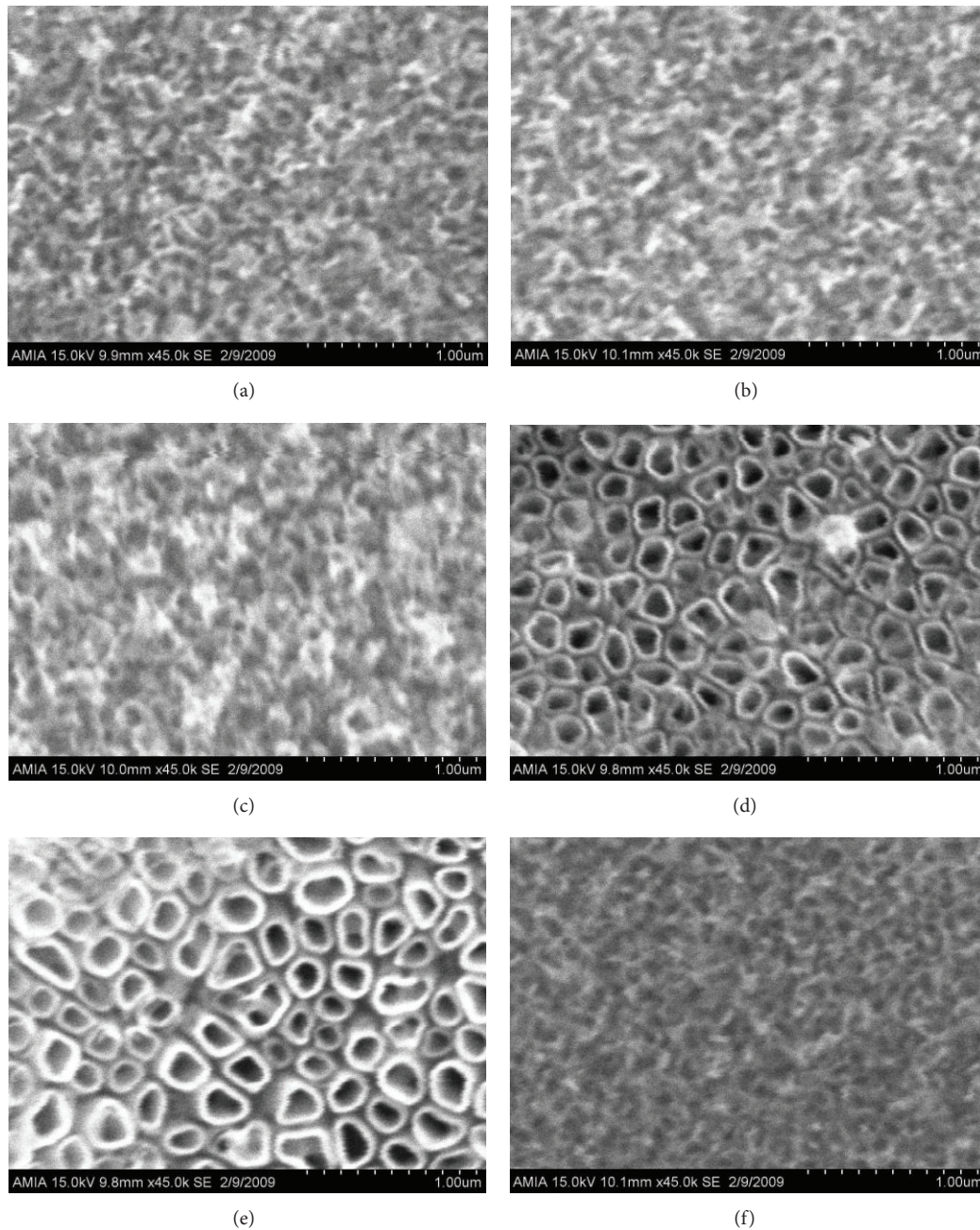
(a)

(b)

(c)

(d)

(e)

(f)

FIGURE 1: Top view of SEM images of TNT synthesized at different weight ratios of glycerol and water: (a) 1 : 9, (b) 2 : 8, (c) 4 : 6, (d) 6 : 4, (e) 8 : 2, and (f) 10 : 0.

were determined at the desired intervals of reaction time by a UV-Vis spectrophotometer (Spectra Academy, K-MAC).

3. Results and Discussion

3.1. Effect of Weight Ratio of Glycerol to Water. Effect of glycerol and water ratio on the dimensions of fabricated TNT is illustrated in Figure 1. Anodization was carried out at 30 V for 2 hours in electrolyte solution containing glycerol, water, and 0.5 wt% NH_4F. The water content in electrolyte solution is 90, 80, 60, 40, 20, and 0%, respectively. Anodization

process was performed at electrolyte solution pH of 6 and bath temperature of 40°C. TiO_2 with tubular structure was observed in glycerol electrolyte with water content of 40 and 20% (Figures 1(d) and 1(e)). Hence, the glycerol/water ratio of 60 : 40% was chosen to perform those anodizations at various anodization voltages, electrolysis time, bath temperature, and electrolyte solution pH. Partially well-formed TNT or collapsed TNT prepared by water contents of 90, 80, 60, and 0% was also shown in Figure 1. The result is consistent with the research finding by Valota et al. [13]. They proposed that electric current densities increases as water content
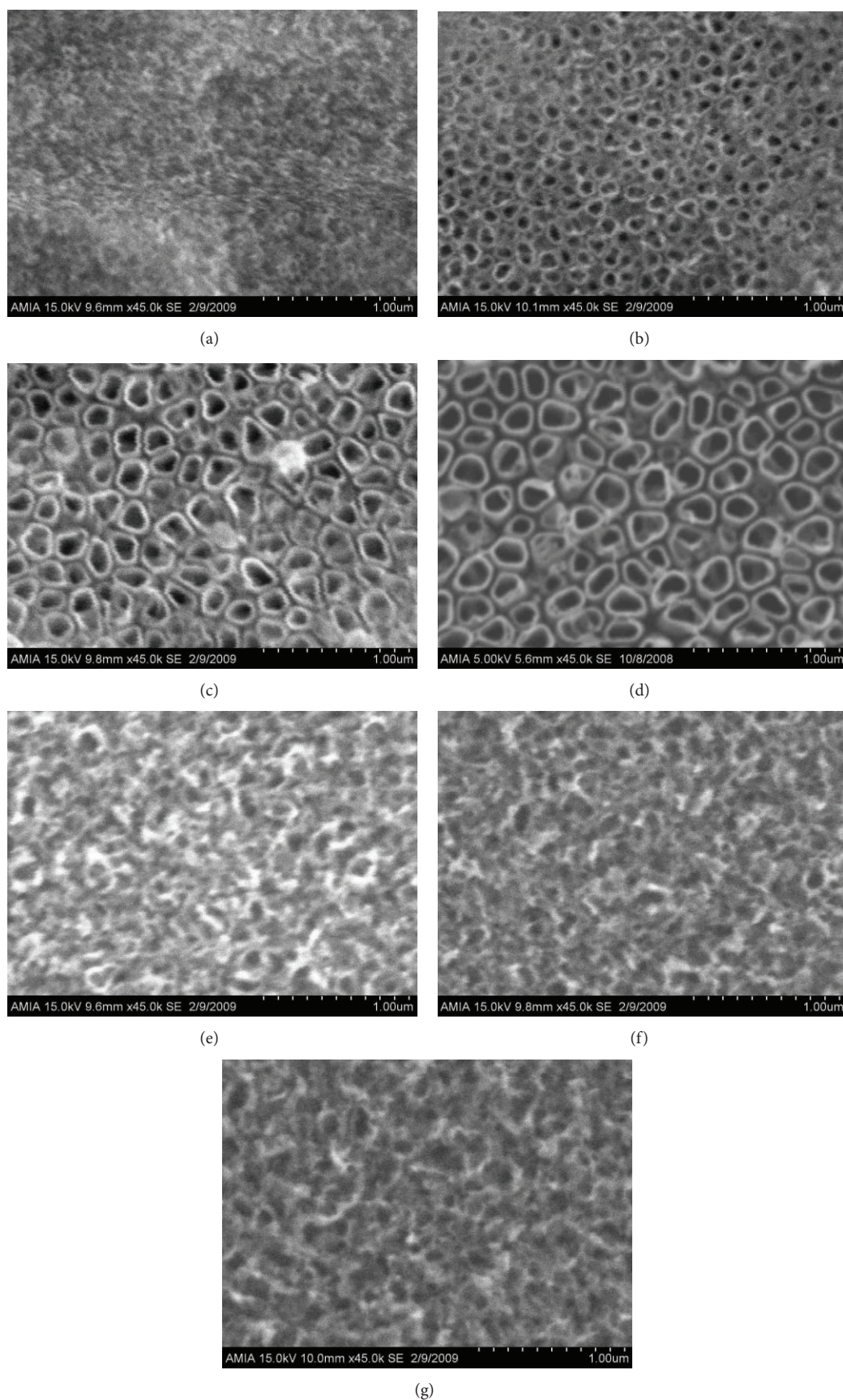
(a)

(b)

(c)

(d)

(e)

(f)

(g)

Figure 2: Top view of SEM images of TNT synthesized at different anodization voltages: (a) 10 V, (b) 20 V, (c) 30 V, (d) 40 V, (e) 50 V, (f) 60 V, and (g) 70 V.
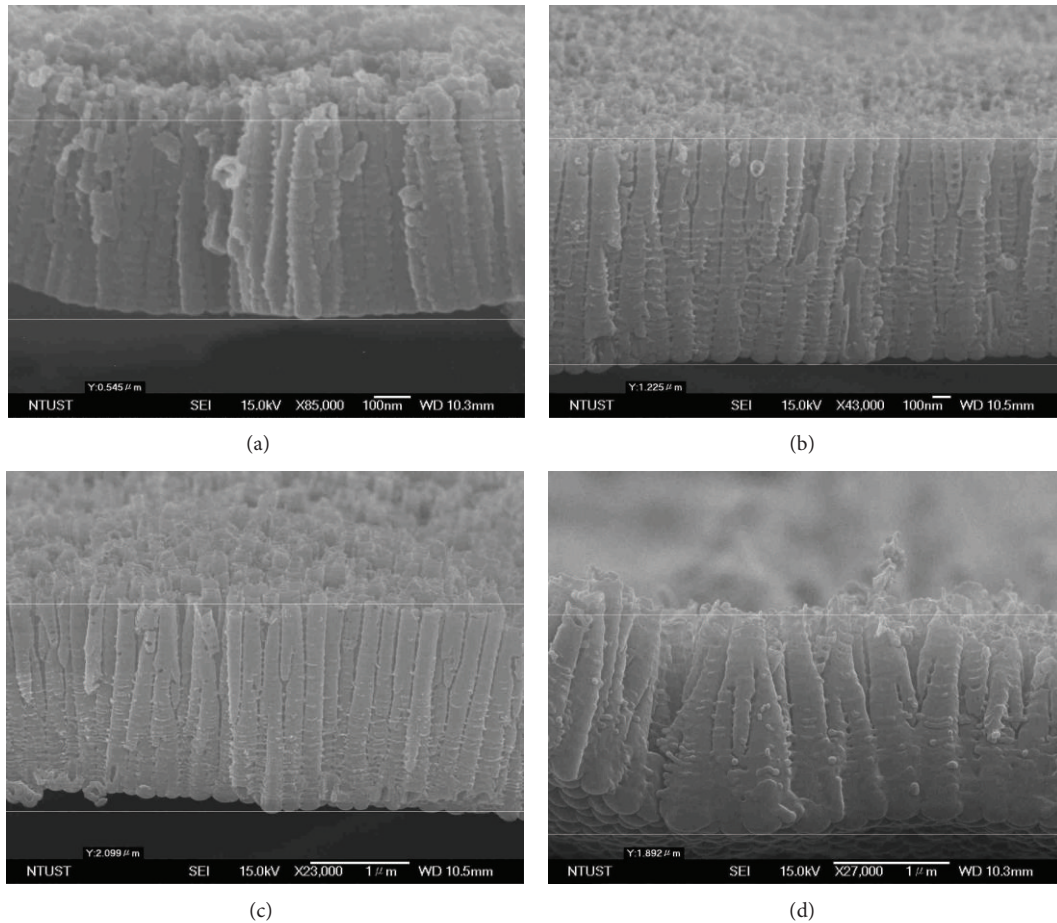
(a)

(b)

(c)

(d)

Figure 3: Front view of SEM images of TNT synthesized at different anodization voltages: (a) 10 V, (b) 20 V, (c) 30 V, and (d) 40 V.

increase and high electric current densities further result in the collapse and dissolve of TNT.

3.2. Effect of Anodization Voltage.

Figure 2 illustrates SEM images for the influence of applied anodization voltage on the fabrication of TiO_2 nanotube arrays. These samples were prepared at water contents of 40 wt% in glycerol containing 0.5 wt% NH_4F, anodization voltage ranged from 10–70 V, electrolysis time of 2 hours, electrolyte solution pH of 6, and bath temperature of 40°C. The TNT structure was observed at applied anodization voltage of 10–40 V but disappeared above 50 V. As shown in Figures 2 and 3, Inner diameter and length of TNT prepared with applied anodization voltage of 10–40 V were determined by SEM cross-section images. Figure 4(a) illustrates that the average inner diameter of TNT was ranged from 50 to 210 nm and increased almost linearly with the increasing applied anodization voltage from 10 to 40 V. Average length of TNT was also linearly increased from 608 to 2100 nm with the increasing applied anodization voltage but decreased above 30 V.

Applied anodization voltage and fluoride concentration in electrolyte solution are proposed to play important roles during anodization to carry out electrochemical oxidation and chemical dissolution reactions. Lee et al. [14] recorded current-time curves during anodization with 20 V at water contents of 30 wt% in glycerol containing different amounts of NH_4F. The current densities increased with increasing the fluoride content in the range of 0–2%. They proposed that the dissolution reaction of the anodic oxide is induced by F^- ions. The growth of TNT is a result of competition between electrochemical oxide formation and chemical dissolution of oxide by fluoride ions. In this study, anodization of Ti foil was conducted in electrolyte solutions containing 0.5 wt% NH_4F, indicating that the chemical dissolution rate of TiO_2 coating was supposed to be roughly the same for all experiments regarding to the anodization of Ti foil, while the electrochemical oxidation rate to form TiO_2 layers was varied with different applied anodization voltages. Hence, the growth of TNT was mainly determined by applied anodization voltage.

Some similar results were reported in the literature. Gong et al. [9] fabricated TNT in 0.5–3.5% HF solutions by applying various anodization voltages. The length of TiO_2 nanotube was approximately 500 nm, and the average inner diameter was 25 to 65 nm. Macak et al. [15] studied the effect of anodization voltage on the fabrication of TNT by anodization in water/glycerol solution (50 : 50 vol%) containing 0.27 M NH_4F. The authors indicated that the inner diameter was linearly increased with increasing anodization voltage.
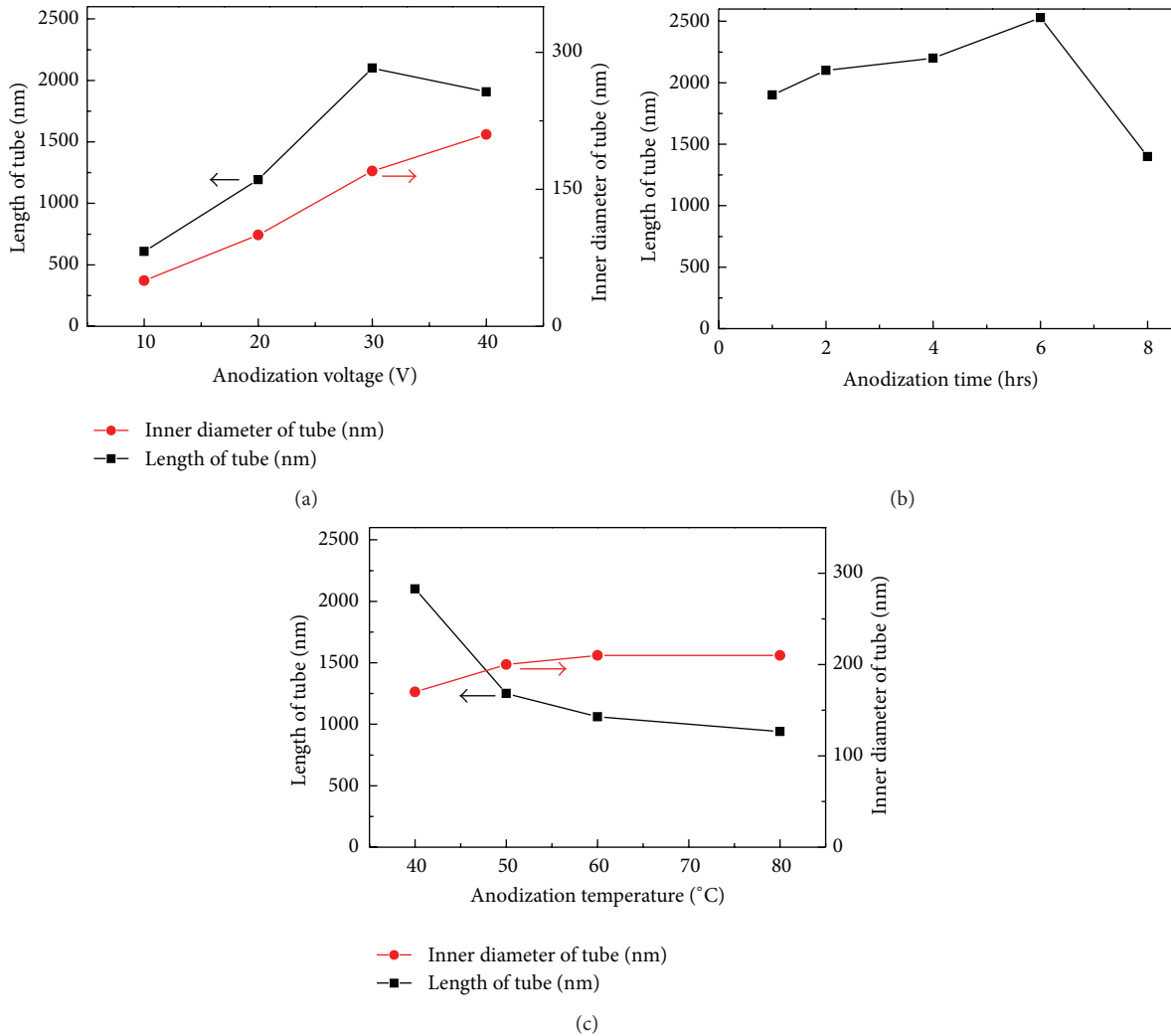
(a)

(b)

(c)

FIGURE 4: Dimensional control of titanium dioxide nanotube arrays with different preparation parameters of (a) anodization voltage, (b) electrocatalysis times, and (c) bath temperature.

The length of TNT fabricated with anodization voltage less than 20 V was found to be increased with anodization voltage and then gradually approached to a constant value with continuously increasing anodization voltage.

3.3. Effect of Electrolysis Time. Figure 5 illustrates SEM images for the influence of electrolysis time ranged from 1 to 10 hours on the fabrication of TiO_2 nanotube arrays. These samples were prepared at water contents of 40 wt% in glycerol containing 0.5 wt% NH_4F, anodization voltage of 30 V, anodization time of 2 hours, electrolyte solution pH of 6, and bath temperature of 40°C. Figures 5 and 4(b) depict the relationship between the dimensions of TNT and electrolysis duration periods. The average length of nanotube increased with increasing anodization time, but the average inner diameter of nanotube was not affected with anodization time for experiments conducted with the same applied anodization voltage. The length of TNT rapidly grew

to 1900 nm at the first hour then was enhanced with growth rate of 126 nm/hour for anodization duration periods from the second to the sixth hour, and thereafter the length of TNT decreased drastically to less than 1400 nm at the eighth hour.

As shown in Figures 5(e) and 5(f), at the eighth hour the length of TNT decreased drastically. At the tenth hour the structure of nanotube arrays could not stay highly ordered and vertically oriented due to collapse of nanotubes. These observations indicate that the anodization of Ti foil has three stages in this study. At the first stage (the first hour), the formation and erosion of titanium dioxide layer arose simultaneously. TNT layer was established initially with a very fast speed. A very high current density at the initial 50 seconds of anodization showed the fast formation of an oxide layer. At the second stage (the second to the sixth hour), the growth of TNT slowed down due to high electric resistance gradually induced by thicker oxide layer; meanwhile, the chemical erosion also slowed down due to the long diffusion path of corrosion agents. The results arose in a slow growing
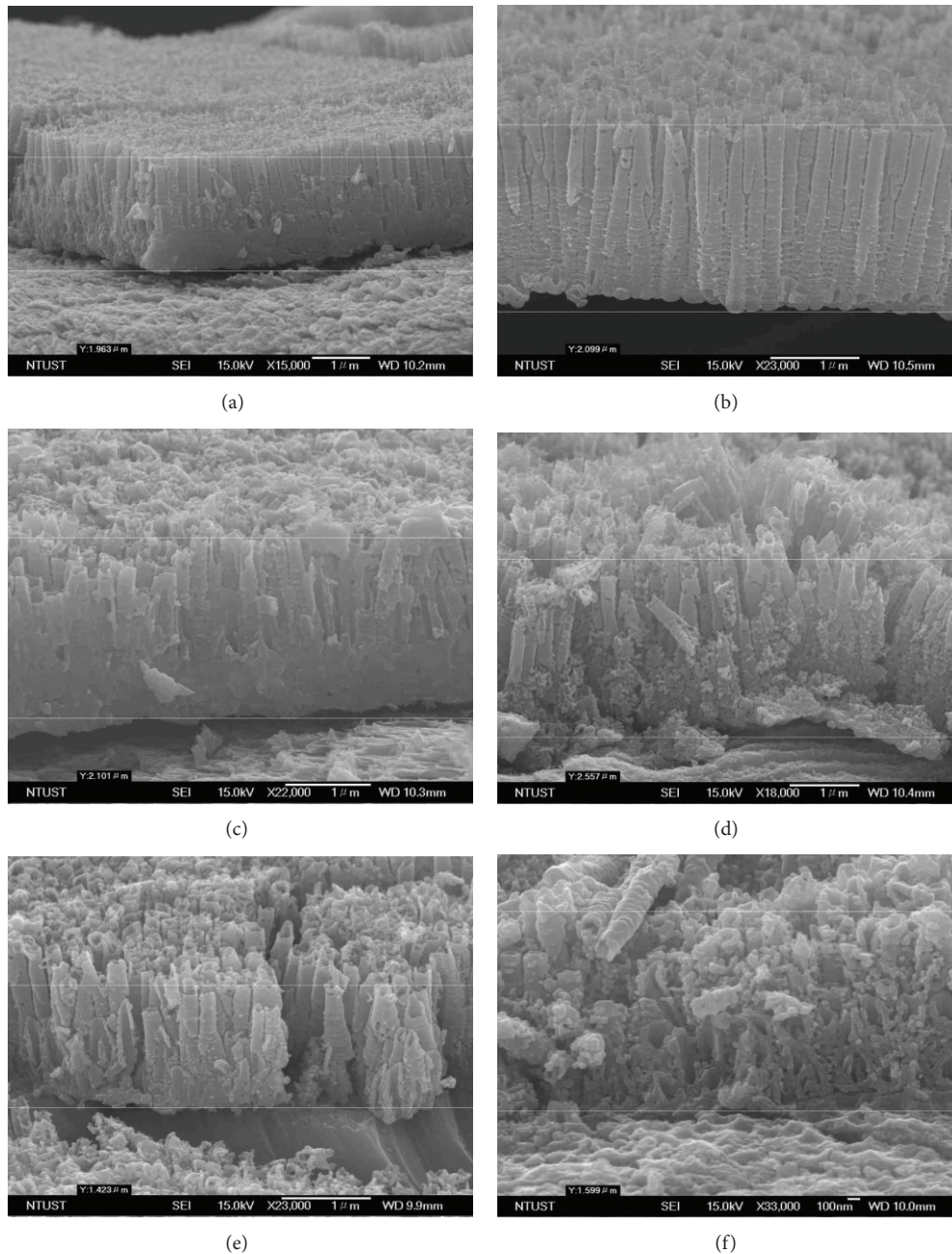
Figure 5: Front view of SEM images of TNT synthesized at different electrocatalysis time: (a) 1 hr, (b) 2 hr, (c) 4 hr, (d) 6 hr, (e) 8 hr, and (f) 10 hr.

rate of nanotubes layer at the second stage. Finally, at the third stage of longer anodization time, the erosion rate was a little faster than the inhibited growth of oxide layer and caused the collapse of nanotubes as anodization time increased. It is assumed that the length of nanotube is continually increased with anodization time until the rates of electrochemical oxidization of Ti foil and chemical dissolution of TiO_2 film reached dynamically equilibrium.

The experimental results are consistent with Cai et al. [16]. With the application of anodization voltage higher than 30 V, the length of TNT was rapidly enhanced with growth rate greater than 300 nm/hour for anodization time less than 4 hours, and thereafter growth rate was decreased drastically to less than 60 nm/hour. For experiments conducted with lower anodization voltages, the length of TNT was gradually increased at steady growth rate of about 40 nm/hour even for anodization time of 12 hours. Normally, the decrease of tube length after a long time of electrolysis in our study (Figure 4(b)) is less reported in the literature. Crawford et al. [17] prepared TNT by anodization in a NaF electrolyte and indicated that the length of TNT increased with increasing anodization time for anodization time less than 2 hours
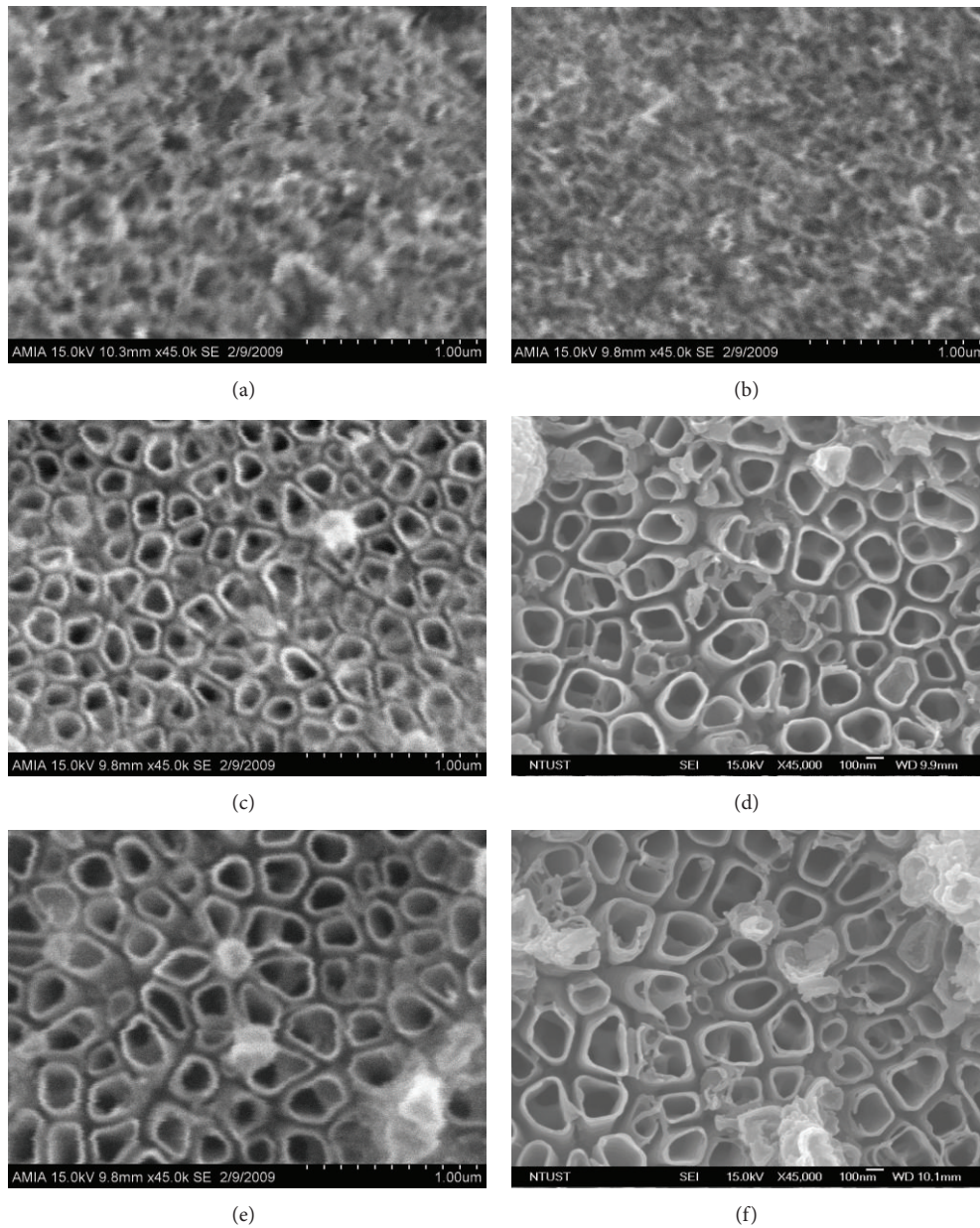
FIGURE 6: Top view of SEM images of TNT synthesized at different bath temperatures: (a) 10°C, (b) 20°C, (c) 40°C, (d) 50°C, (e) 60°C, and (f) 80°C.

and remained constant thereafter. Macak and Schmuki [18] and Kim et al. [19] examined the effect of anodization time on the dimension of TNT and revealed that the tube diameter and wall thickness were not varied with anodization time.

3.4. Effect of Bath Temperature. Effect of bath temperature on the dimensions of fabricated TNT is illustrated in Figures 6 and 7. These samples were prepared at water contents of 40 wt% in glycerol containing 0.5 wt% NH_4F, bath temperature ranged from 10 to 80°C, anodization voltage of 30 V for 2 hours, and electrolyte solution pH of 6. The TNT was observed at bath temperature ranged from 80 to 40°C but disappeared below 20°C. As shown in Figure 4(c), inner

diameter and length of TNT prepared with bath temperature from 40 to 80°C were determined by SEM cross-section images. Figure 4(c) showed that average inner diameter of TNT increased from 170 to 210 nm as bath temperature increased from 40 to 50°C but had comparable diameters as bath temperature was above 50°C. Average length of TNT was inversely decreased from 2100 to 940 nm with increasing bath temperature but had comparable lengths as bath temperature was above 60°C.

Unlike anodization voltage and electrolysis time, the effects of bath temperature and electrolyte solution pH only attracted a few researchers' attention. Lim et al. [20] examined the effect of bath temperature on the dimension of TNT
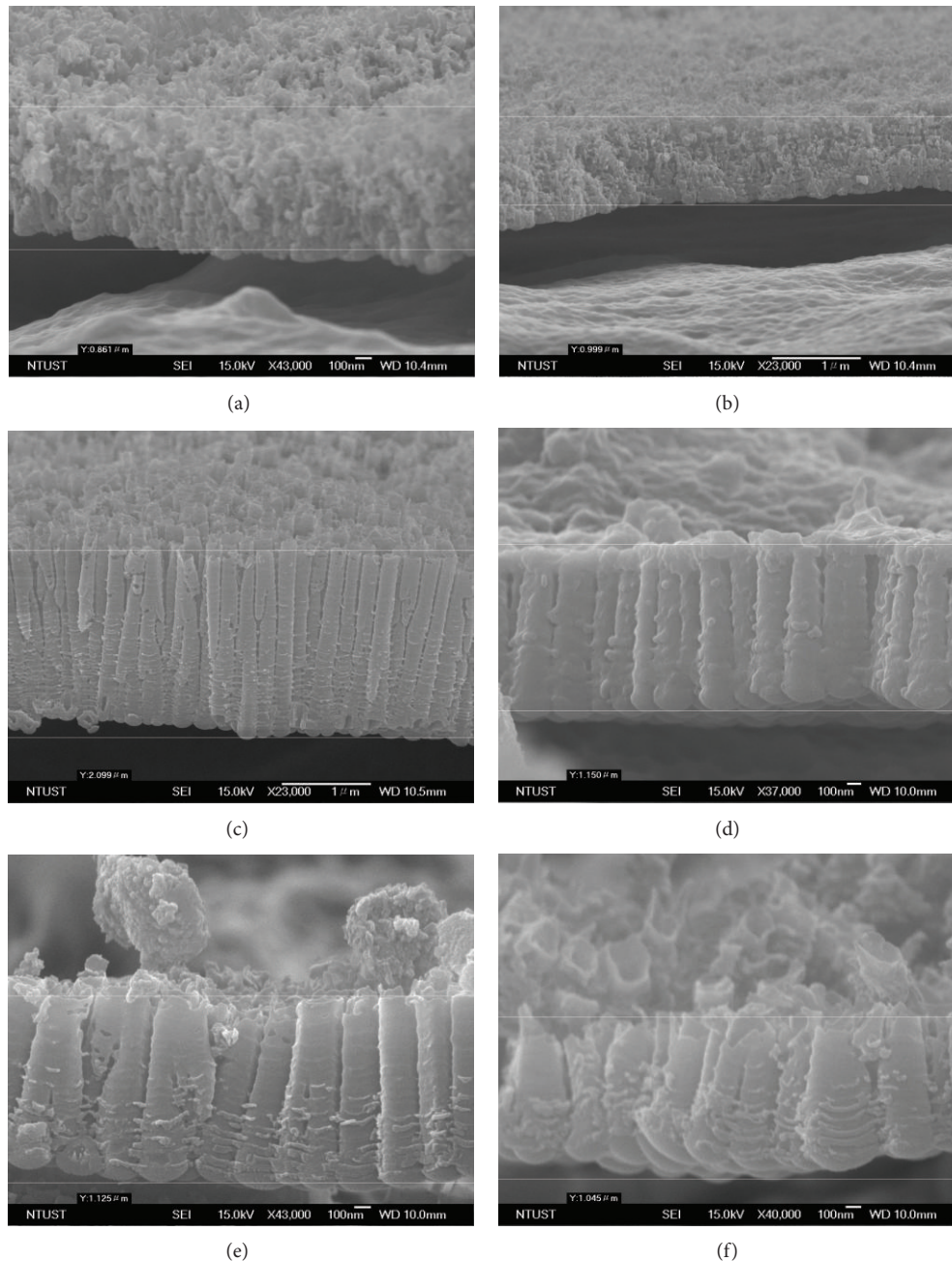
(a)

(b)

(c)

(d)

(e)

(f)

Figure 7: Front view of SEM images of TNT synthesized at different bath temperatures: (a) 10°C, (b) 20°C, (c) 40°C, (d) 50°C, (e) 60°C, and (f) 80°C.

and found that TNT can still be fabricated at 35°C; however, the tube length decreases whereas tube diameter increases with elevated temperature from 10 to 35°C. Some different results were reported by various studies. Macak and Schmuki [18] anodized Ti in mixture of glycerol and water (50 : 50) containing 0.5 wt% NH_4F at various bath temperatures of 20, 40, 60, and 80°C with 20 V for 6 hours. Their result showed that the length of TNT increased as bath temperature increased.

There are some differences between the literature and our study including electrolyte composition, anodization voltage, and electrolysis time, and therefore the results of these studies are different. It appears that TNT could form at low bath temperature for a longer electrolysis time, but our study performs 2 hours of electrolysis time and only gets a random oxide layer. On other hands, our result is consistent with the study of Mor et al. [21]. They studied the TNT prepared at different bath temperatures by 10 V anodization in an electrolyte of 0.5% HF and acetic acid mixed in a 7 : 1 ratio. The result shows that the length of the nanotubes increases from 120 nm to 224 nm with decreasing bath temperature from 50°C to 5°C. The electric density
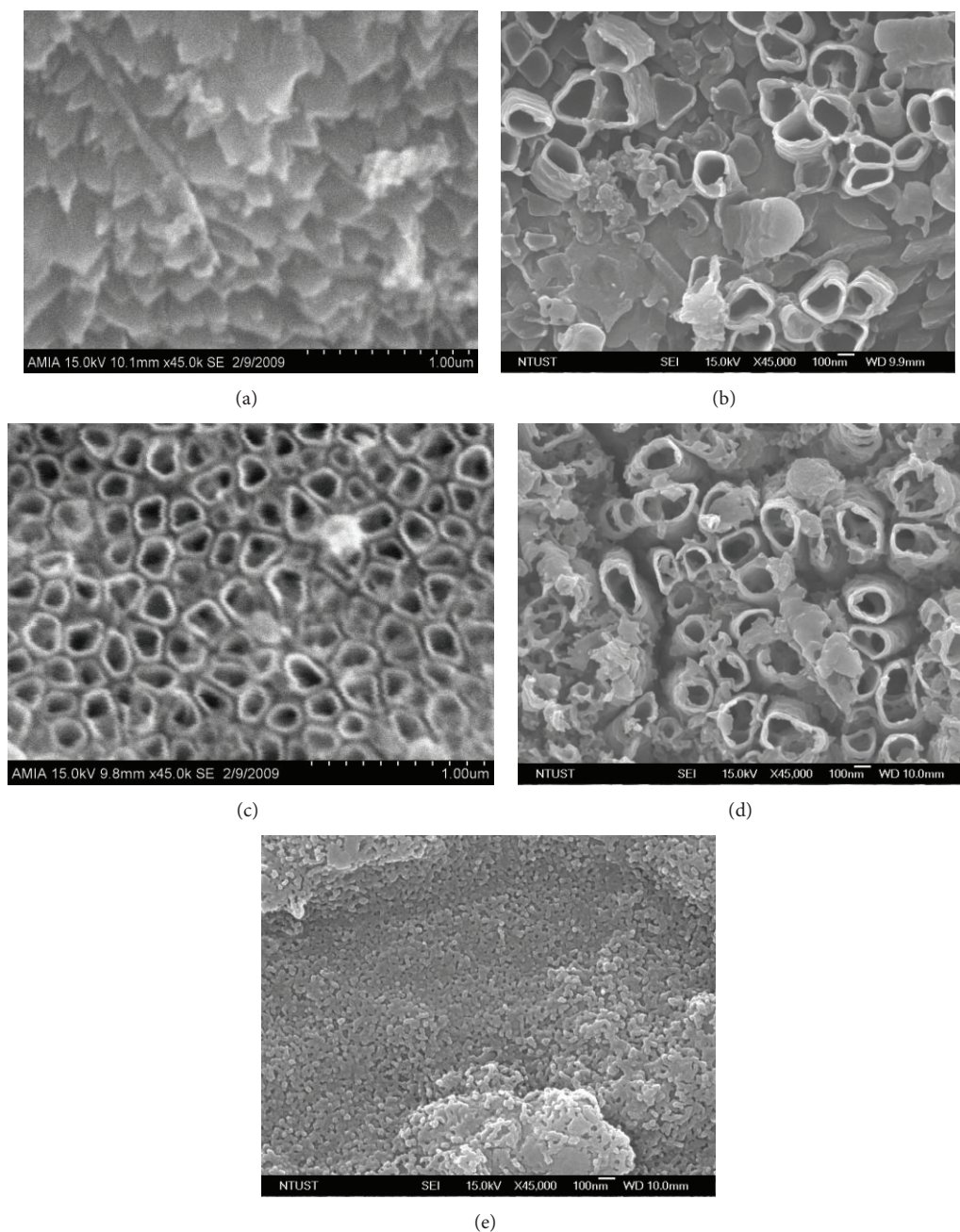
(a)

(b)

(c)

(d)

(e)

FIGURE 8: Top view of SEM images of TNT synthesized at different electrolyte solution pH: (a) 2, (b) 4, (c) 6, (d) 8, and (e) 10.

of anodization bath will increase with rising bath temperature. At the same time, the electric field formed in titanium anode will also increase. High electric current density and appropriate chemical etching will match up and make a fast transform of oxidize layer to nanotubes at the initial oxidizing stage. The nanotubes formed in this situation got a bigger diameter and a longer length.

3.5. Effect of Electrolyte Solution pH.

Figure 8 illustrates SEM images for the influence of electrolyte solution pH on the fabrication of TiO_2 nanotube arrays. These samples were

prepared at water contents of 40 wt% in glycerol containing 0.5 wt% NH_4F, electrolyte solution pH ranged from 2 to 10, anodization voltage of 30 V for 2 hours, and bath temperature of 40°C. The results showed that a flaky layer was formed at pH 2 (Figure 8(a)). Nanotube structure is produced at PH 4, but nanotube was not formed around the entire Ti foil. There was some flaky oxidizing layer structure disperses behind the nanotube structure (Figure 8(b)). At PH 6, well-defined and highly ordered TNT was formed (Figure 8(c)). At PH 8, nanotube structure was not well developed (Figure 8(d)). At PH 10, a fine concave and convex porous surface was formed (Figure 8(e)). Electrolyte solution pH influences oxidation
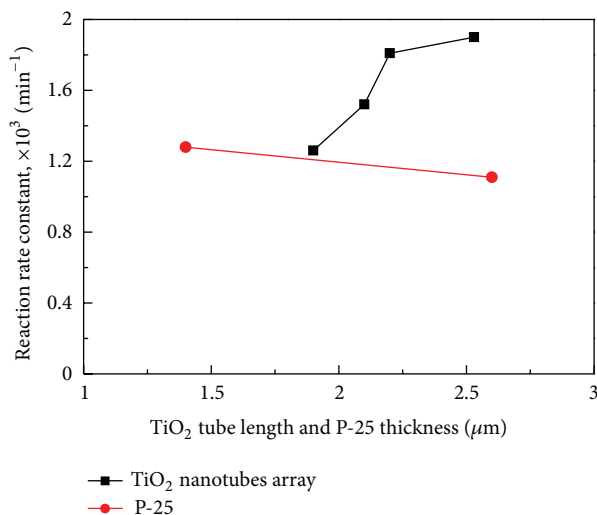
FIGURE 9: Photocatalytic reaction rate constants of TiO_2 nanotube arrays film and P-25 film as a function of film thickness.

rate and chemical etching rate of oxidizing layer. It will further control the surface morphology of TiO_2 film and whether TNT will be formed or not.

At too low pH, chemical etching rate of fluorine ion was too big. Drastic chemical etching on surface resulted in a deep flaky layer, and TNT was unable to be formed. As electrolyte solution pH roses gradually, oxidation and chemical etching rates reached a dynamic equilibrium and promoted the form of TNT. At too high pH, oxidation rate of titanium slowed down but the chemical etching rate slowed down even more and resulted in a concave and convex porous surface. Macák et al. [22] proposed that transition and diffusion of H^+ ion at low pH resulted in acidic solution accumulated in the bottom of concave. Chemical etching of the accumulated acidic solution caused a deep flaky layer. Cai et al. [16] proposed that high pH caused a low oxidation rate. It needs much time to establish the dynamic equilibrium between oxidation of titanium and chemical etching of oxide layer.

3.6. Comparison of Rate Constants for TNT Film and P-25 Film. This study compared the effect of thicknesses of TNT film and P-25 film on the photocatalysis rates of methylene blue. Figure 9 showed the photocatalytic reaction rate constants of 10 mg/L methylene blue with comparable thicknesses of TNT film and P-25 film under illumination of UV-LED in a recirculation flow system as described in Experimental section. The photocatalytic reaction rate constants with TNT film thicknesses of 1900, 2100, 2200, 2530 nm are 1.26×10^{-3}, 1.52×10^{-3}, 1.81×10^{-3}, and 1.90×10^{-3} min^{-1}, respectively. As lengths of TNT increased the reaction rate constants increased, but the enhancement was retarded when the length of TNT reaching 2200 nm appeared to be the limited penetration of incident UV light. The photocatalytic reaction rate with TNT film was higher than P-25 film at above the film thicknesses range.
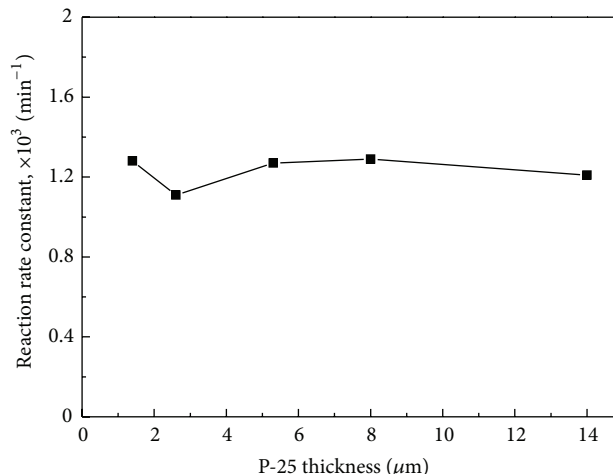

FIGURE 10: Photocatalytic reaction rate constants of different thicknesses of P-25 film ranged from 1400 to 14000 nm.

This result is similar to Macak et al.'s [23]. They prepared TNT film with different tube lengths of 500, 2500, and 4500 nm to study photocatalytic reaction of methylene blue and acid orange 7. The result showed that the photocatalytic reaction ratio is better for TNT films than 2500 nm thickness of P-25 film. Furthermore, the photocatalytic reaction ratio had a positive dependence on the length of nanotubes. Wu et al. [24] studied the photoelectrocatalytic degradation of methylene blue. A reaction rate constant of 2.97×10^{-3} min^{-1} was observed at a low bias level of 0.6 V. Because of the electric field enhancement, the reaction constant of photoelectro-catalysis is bigger than that of our study on photocatalysis. As shown in Figure 10, the photocatalytic reaction rate constants of different thicknesses of P-25 film ranging from 1400 to 14000 nm had no obvious variation. It could be proposed that only the top layer of particle-packed P-25 film contacts with dye solution and results in photocatalytic reaction. Other P-25 below the top layer has no contribution to photocatalysis. On other hand, because of the porous structure of TNT film, the dye solution has more opportunities to contact with TiO_2. The porous nanotube structure causes the photocatalysis rate constants to increase as the lengths of TNT increase.

4. Conclusion

In summary, self-organized TNT films were synthesized using anodization method in NH_4F containing electrolyte. The growth of TNT was mainly determined by applied anodization voltage rather than bath temperature. The inner diameter of TNT was mainly determined by the anodization voltage while the length of TNT was affected by both anodization voltage, and anodization time. With the photocatalysis of methylene blue, It was found that the best well-defined, highly ordered, and uniformed TNT film was prepared in glycerol electrolyte with water content of 40%, anodization voltage of 30 V, electrolysis time of 6 hours, bath temperature of 40°C, and electrolyte solution pH of 6. The photocatalytic reaction rate constants with TNT film thicknesses ranged from 1900
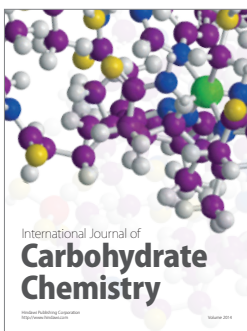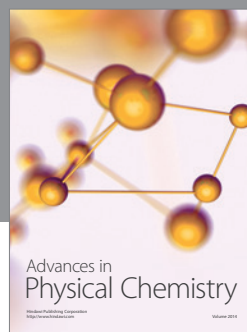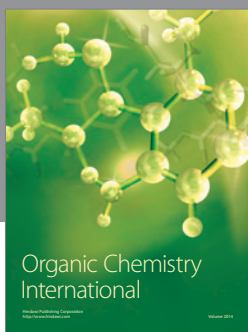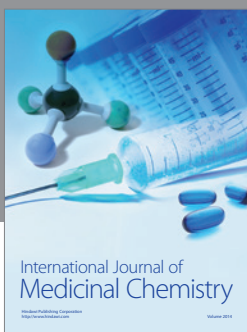
to 2530 nm were higher than with P-25 film at comparable thicknesses.

Acknowledgment

References

[1] D. M. Blake, "Bibliography of work on the heterogeneous photocatalytic removal of hazardous compounds from water and air," Tech. Rep., U.S. National Renewable Energy Laboratory, Golden, Colo, USA, 2001.

[2] A. Fujishima and K. Honda, "Electrochemical photolysis of water at a semiconductor electrode," *Nature*, vol. 238, no. 5358, pp. 37–38, 1972.

[3] A. L. Linsebigler, G. Lu, and J. T. Yates, "Photocatalysis on TiO_2 surfaces: principles, mechanisms, and selected results," *Chemical Reviews*, vol. 95, no. 3, pp. 735–758, 1995.

[4] J. M. Macák, H. Tsuchiya, A. Ghicov, and P. Schmuki, "Dye-sensitized anodic TiO_2 nanotubes," *Electrochemistry Communications*, vol. 7, no. 11, pp. 1133–1137, 2005.

[5] X. Quan, X. Ruan, H. Zhao, S. Chen, and Y. Zhao, "Photoelectrocatalytic degradation of pentachlorophenol in aqueous solution using a TiO_2 nanotube film electrode," *Environmental Pollution*, vol. 147, no. 2, pp. 409–414, 2007.

[6] N. Wang, X. Li, Y. Wang, X. Quan, and G. Chen, "Evaluation of bias potential enhanced photocatalytic degradation of 4-chlorophenol with TiO_2 nanotube fabricated by anodic oxidation method," *Chemical Engineering Journal*, vol. 146, no. 1, pp. 30–35, 2009.

[7] P. Hoyer, "Formation of a titanium dioxide nanotube array," *Langmuir*, vol. 12, no. 6, pp. 1411–1413, 1996.

[8] T. Kasuga, M. Hiramatsu, A. Hoson, T. Sekino, and K. Niihara, "Formation of titanium oxide nanotube," *Langmuir*, vol. 14, no. 12, pp. 3160–3163, 1998.

[9] D. Gong, C. A. Grimes, O. K. Varghese et al., "Titanium oxide nanotube arrays prepared by anodic oxidation," *Journal of Materials Research*, vol. 16, no. 12, pp. 3331–3334, 2001.

[10] G. K. Mor, O. K. Varghese, M. Paulose, K. Shankar, and C. A. Grimes, "A review on highly ordered, vertically oriented TiO_2 nanotube arrays: fabrication, material properties, and solar energy applications," *Solar Energy Materials and Solar Cells*, vol. 90, no. 14, pp. 2011–2075, 2006.

[11] Y. Alivov and Z. Y. Fan, "Efficiency of dye sensitized solar cells based on TiO_2 nanotubes filled with nanoparticles," *Applied Physics Letters*, vol. 95, no. 6, Article ID 063504, 2009.

[12] W. Y. Wang and Y. Ku, "Photocatalytic degradation of reactive red 22 in aqueous solution by UV-LED radiation," *Water Research*, vol. 40, no. 12, pp. 2249–2258, 2006.

[13] A. Valota, D. J. LeClere, P. Skeldon et al., "Influence of water content on nanotubular anodic titania formed in fluoride/glycerol electrolytes," *Electrochimica Acta*, vol. 54, no. 18, pp. 4321–4327, 2009.

[14] B. G. Lee, J. W. Choi, S. E. Lee, Y. S. Jeong, H. J. OH, and C. S. Chi, "Formation behavior of anodic TiO_2 nanotubes in fluoride containing electrolytes," *Transactions of Nonferrous Metals Society of China*, vol. 19, no. 4, pp. 842–845, 2009.

[15] J. M. Macak, H. Hildebrand, U. Marten-Jahns, and P. Schmuki, "Mechanistic aspects and growth of large diameter self-organized TiO_2 nanotubes," *Journal of Electroanalytical Chemistry*, vol. 621, no. 2, pp. 254–266, 2008.

[16] Q. Cai, M. Paulose, O. K. Varghese, and C. A. Grimes, "The effect of electrolyte composition on the fabrication of self-organized titanium oxide nanotube arrays by anodic oxidation," *Journal of Materials Research*, vol. 20, no. 1, pp. 230–236, 2005.

[17] G. A. Crawford, N. Chawla, K. Das, S. Bose, and A. Bandyopadhyay, "Microstructure and deformation behavior of biocompatible TiO_2 nanotubes on titanium substrate," *Acta Biomaterialia*, vol. 3, no. 3, pp. 359–367, 2007.

[18] J. M. Macak and P. Schmuki, "Anodic growth of self-organized anodic TiO_2 nanotubes in viscous electrolytes," *Electrochimica Acta*, vol. 52, no. 3, pp. 1258–1264, 2006.

[19] E. Y. Kim, J. H. Park, and G. Y. Han, "Design of TiO_2 nanotube array-based water-splitting reactor for hydrogen generation," *Journal of Power Sources*, vol. 184, no. 1, pp. 284–287, 2008.

[20] Y. C. Lim, Z. Zainal, W. T. Tan, and M. Z. Hussein, "Anodization parameters influencing the growth of titania nanotubes and their photoelectrochemical response," *International Journal of Photoenergy*, vol. 2012, Article ID 638017, 9 pages, 2012.

[21] G. K. Mor, K. Shankar, M. Paulose, O. K. Varghese, and C. A. Grimes, "Enhanced photocleavage of water using titania nanotube arrays," *Nano Letters*, vol. 5, no. 1, pp. 191–195, 2005.

[22] J. M. Macák, H. Tsuchiya, and P. Schmuki, "High-aspect-ratio TiO_2 nanotubes by anodization of titanium," *Angewandte Chemie*, vol. 44, no. 14, pp. 2100–2102, 2005.

[23] J. M. Macak, M. Zlamal, J. Krysa, and P. Schmuki, "Self-organized TiO_2 nanotube layers as highly efficient photocatalysts," *Small*, vol. 3, no. 2, pp. 300–304, 2007.

[24] X. Wu, Z. Huang, Y. Liu, and M. Fang, "Investigation on the photoelectrocatalytic activity of well-aligned TiO_2 nanotube arrays," *International Journal of Photoenergy*, vol. 2012, Article ID 832516, 7 pages, 2012.